

# Discovery of X-Ray Burst Oscillations from a Neutron-Star X-Ray Transient in the Globular Cluster NGC 6440

P. Kaaret

*Harvard-Smithsonian Center for Astrophysics, 60 Garden St., Cambridge, MA 02138, USA*  
pkaaret@cfa.harvard.edu

J.J.M. in 't Zand and J. Heise

*SRON National Institute for Space Research, Sorbonnelaan 2, 3584 CA Utrecht, the Netherlands*  
*Astronomical Institute, Utrecht University, P.O. Box 80 000, 3508 TA Utrecht, the Netherlands*

J.A. Tomsick

*Center for Astrophysics and Space Sciences, Code 0424, 9500 Gilman Drive,*  
*University of California at San Diego, La Jolla, CA 92093*

## ABSTRACT

We report the discovery of millisecond oscillations in an X-ray burst from the X-ray transient SAX J1748.9-2021 in the globular cluster NGC 6440. Oscillations at a frequency of  $409.7 \pm 0.3$  Hz were present in one of nine X-ray bursts observed with the Proportional Counter Array on the Rossi X-ray Timing Explorer during the outburst which occurred in 2001. The burst was one of the two dimmest and had the longest duration and decay time. The average peak luminosity of two bursts showing radius expansion is  $(3.6 \pm 0.4) \times 10^{38}$  ergs $^{-1}$ , consistent with the Eddington luminosity for a  $1.4M_{\odot}$  and 10 km radius neutron star burning hydrogen-poor matter. We speculate that the dichotomy observed between sources with burst oscillations at once versus twice the frequency difference of kHz quasiperiodic oscillations in the persistent emission may be related to the magnetic field geometry of the neutron stars.

*Subject headings:* Galaxy: globular clusters: individual (NGC 6440) — stars: neutron — X-rays: binaries — stars: individual (SAX J1748.9-2021)

## 1. Introduction

The discovery of millisecond oscillations in thermonuclear X-ray bursts provided the first direct measurements of the spin frequencies of neutron stars in low-mass X-ray binaries (LMXBs) (Strohmayer et al. 1996; Strohmayer & Markwardt 2002). The presence of neutron stars rotating with millisecond periods in NS-LMXBs was suggested more than a decade previously (Alpar et al. 1982) and is key in understanding the relation of LMXBs and millisecond radio pulsars.

X-ray burst oscillation sources form two distinct classes: “fast oscillators” with frequencies

close to twice the frequency difference of the kHz quasiperiodic oscillations (QPOs) seen in the persistent emission, and “slow oscillators” with frequencies near the difference of the kHz QPO frequencies (White & Zhang 1997). If the kHz QPO frequency difference is close to the spin frequency of the neutron star, then the slow oscillators have a burst oscillation frequency close to the spin frequency, while the fast oscillators produce signals at twice the spin frequency. The fast oscillators produce burst oscillations predominately, but not exclusively, in photospheric radius expansion bursts, while the slow oscillators produce os-

cillations in bursts both with and without photospheric radius expansion (Muno et al. 2001). This indicates that the difference between the two classes is a physical difference and not a selection effect. The nature of this physical difference is unknown.

If the fast oscillators indicate twice the spin frequency and the slow oscillators indicate the spin frequency, then the spin frequency distribution of neutron stars in X-ray bursters is clustered with a maximum value near 400 Hz. Clustering in the spin frequency distribution has been variously interpreted as evidence for very efficient mass ejection by rapidly rotating neutron stars in binaries (Burderi et al. 2001), a gravitational radiation limit on the spin-up of accreting neutron stars (Bildsten 1998) and for the existence of a phase change in superdense nuclear matter (Glendenning & Weber 2001).

Increasing the sample of sources from which burst oscillations are detected is crucial for determining the physical nature of the difference between the fast and slow oscillators and in accurately measuring the spin frequency distribution of neutron stars in LMXBs. Here, we describe observations made with the Rossi X-Ray Timing Explorer (RXTE; Bradt, Rothschild, & Swank 1993) following the detection of X-ray bursts from the transient source SAX J1748.9-2021 located in the globular cluster NGC 6440. We report the discovery of millisecond oscillations in one X-ray burst. Because the source is located in a globular cluster, the distance is known and accurate luminosities can be calculated. We find that the peak luminosity of the radius expansion bursts is consistent with the Eddington limit for a  $1.4M_{\odot}$  and 10 km radius neutron star with hydrogen-poor matter. We describe the source and our observations in §2, the X-ray bursts in §3, the persistent emission in §4, and conclude in §5 with a few comments on the nature of the difference between the fast and slow X-ray burst oscillators.

## 2. Observations of NGC 6440

NGC 6440 is a globular cluster at a distance of  $8.5 \pm 0.4$  kpc (Ortolani, Barbuy, & Bica 1994) and located near the Galactic center. Bright, transient X-ray emission coincident with NGC 6440 was first detected with OSO-7 and UHURU in December

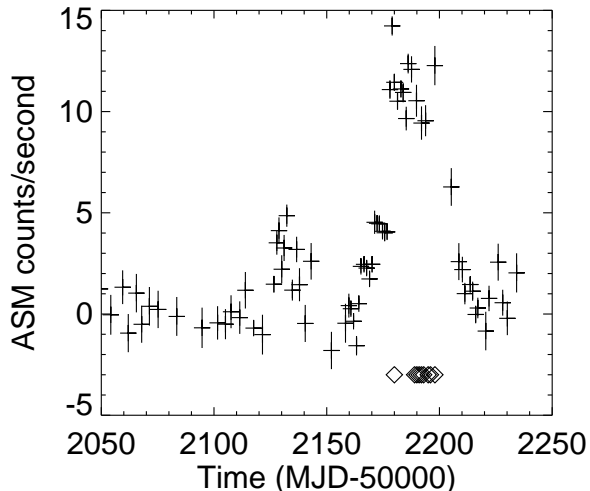


Fig. 1.— RXTE/ASM light curve of the 2001 outburst from NGC 6440. The points are one day averages of the ASM count rates. The diamonds indicate the times of the PCA observations.

1971 (Markert et al. 1975; Forman, Jones, Tananbaum 1976). Strong X-ray outbursts were found, again, in August 1998 (in 't Zand et al. 1999) and August 2001 (in 't Zand et al. 2001). The peak luminosities of the outbursts were near  $10^{37}$  erg s $^{-1}$ . The durations of the outbursts were from one to a few months. The 1998 and 2001 outbursts are from the same object (in 't Zand et al. 2001) identified with the optical star referred to as V2 in (Verbunt et al. 2000). Whether the 1971 outburst is from the same object or one of the other, currently quiescent, LMXBs in NGC 6440 (Pooley et al. 2002) is unknown. Type-I X-ray bursts detected in 1998 and 2001 with the Wide-Field Camera (WFC) on BeppoSAX and a high resolution image of the cluster obtained with Chandra while the source was active during 2001 clearly identify the source SAX J1748.9-2021 with V2 and as an accreting neutron star (in 't Zand et al. 2001).

The RXTE All-Sky Monitor (ASM) light curve of the 2001 outburst is shown in Fig. 1. The outburst started around MJD 52129 (8 August 2001), as reported by the MIT ASM team. This initial event was relatively weak at its peak and lasted only 12 days. After a pause of about 20 days, NGC 6440 again became bright in x-rays. The x-ray emission rose gradually over about 10 days and then jumped rapidly to the peak flux level

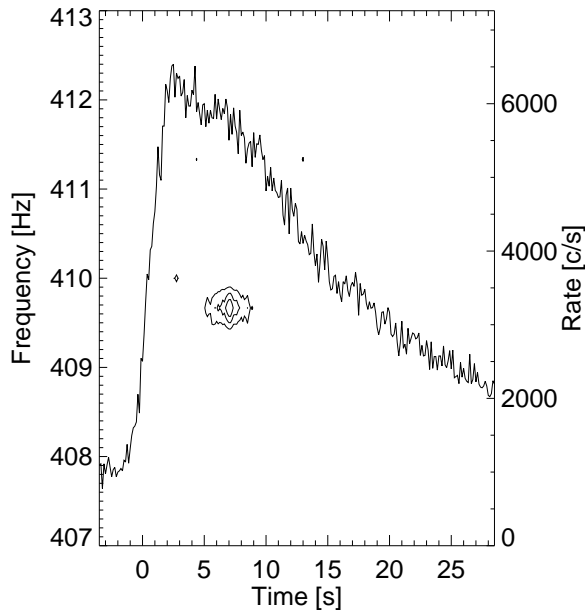


Fig. 2.— Dynamical power spectrum of burst 9 with the burst light curve (count rate) superimposed. The contours are at Leahy powers of 12, 20, and 28. The contours are generated from power spectra for overlapping 3 s intervals of data with the power plotted at the mid-point of the interval. The left vertical axis gives frequency values for the contours. The right axis gives count rates, for the sum of the 3 PCUs on during the burst, for the light curve.

near 12 ASM c/s, which corresponds to a flux near  $3.2 \times 10^{-9} \text{ erg cm}^{-2} \text{ s}^{-1}$  in the 2–10 keV band or a luminosity of  $3 \times 10^{37} \text{ erg s}^{-1}$  for a source located at the distance of NGC 6440. High flux levels persisted for about 20 days, and then the source rapidly declined and became undetectable with the ASM.

The X-ray bursts found with the WFC during the 2001 outburst triggered an RXTE Target-of-Opportunity program which led to an observation on 2001 September 28 and multiple observations during October 7–16. The total observation time was 81 ks. Our observations occurred during the bright phase of the outburst and in the initial part of the final decline. Data were obtained from the Proportional Counter Array (PCA) in the same spectral and timing modes described in Kaaret et al. (2002).

### 3. X-Ray Bursts

We used the Standard 1 data which has 0.125 s time resolution and no energy information to search for X-ray bursts and found nine bursts, see Table 1. We extracted energy spectra for the bursts from event mode data with 64 channels of energy resolution using all Proportional Counter Units (PCUs) on during each burst and all layers. We include data from PCU0 because the problems with background rejection and modeling caused by the loss of its propane layer are not important for spectral analysis of these relatively bright bursts. We note that we did use the most recent response matrices, which include a correction for the spectral response due to the loss of the propane layer. Spectra were accumulated for 0.25 s intervals and corrected for deadtime effects. A spectrum from 10 s of data preceding each burst was subtracted to eliminate the contribution of the persistent emission.

We fitted the resulting spectra in the 3–20 keV band with an absorbed blackbody model with the column density fixed to  $5.9 \times 10^{21} \text{ cm}^{-2}$ , the value equivalent to the optical reddening (Pooley et al. 2002). The results are shown in Table 1. The bolometric flux was calculated from the spectral fit. The equivalent blackbody radius quoted in the table was calculated assuming a distance of 8.5 kpc and the uncertainty does not reflect the distance uncertainty. We note that these characterizations are only approximate since significant deviations from blackbody spectra have been detected from some sources and reprocessing of the radiation in the neutron star atmosphere alters the observed temperature and inferred radius from the true values (Lewin et al. 1995).

Bursts 1 and 5 show evidence for radius expansion including a sharp increase in radius of more than 20 km and a simultaneous decrease in temperature of more than 0.7 keV. The peak fluxes for these two bursts are consistent within the errors and their average peak luminosity is  $(4.3 \pm 0.5) \times 10^{38} \text{ erg s}^{-1}$  where the uncertainty includes the distance uncertainty. The fluxes reported from the RXTE PCA with PCUs 0, 1, 2, and 3 operating (which was the case during bursts 1 and 5) are systematically a factor of 1.2 higher than from other instruments. Assuming that this factor represents an error in the abso-

	Time	Peak Flux ( $10^{-8} \text{ erg cm}^{-2} \text{ s}^{-1}$ )	Peak Radius (km)	Decay Time (s)	Duration (s)
1	Oct 8 at 09:20:50	$5.1 \pm 0.5$	$48.3 \pm 1.2$	3.7	11
2	Oct 8 at 11:15:05	$3.8 \pm 0.5$	$14.3 \pm 0.9$	3.9	12
3	Oct 10 at 06:25:36	$4.6 \pm 0.5$	$19.9 \pm 1.3$	4.3	12
4	Oct 10 at 09:25:03	$2.5 \pm 0.4$	$9.1 \pm 1.1$	9.4	24
5	Oct 11 at 07:49:37	$4.8 \pm 0.5$	$23.5 \pm 1.5$	3.9	11
6	Oct 11 at 09:40:37	$3.6 \pm 0.5$	$12.7 \pm 0.9$	6.6	18
7	Oct 13 at 07:43:35	$3.7 \pm 0.5$	$18.1 \pm 1.4$	4.4	14
8	Oct 16 at 04:58:12	$4.0 \pm 0.6$	$9.3 \pm 0.7$	6.8	21
9	Oct 16 at 08:40:28	$2.5 \pm 0.4$	$8.5 \pm 0.9$	13.0	36

Table 1: Properties of X-Ray Bursts. The table gives for each burst: the time (UTC) in the year 2001 at the start the burst, the bolometric peak flux, the maximum blackbody radius, the  $1/e$ -folding time in the tail of the decay, and the duration defined as the interval over which the flux is greater than 10% of the peak flux.

lute calibration of the PCA (Tomsick et al. 1999), we reduce the flux by this factor and find an average peak luminosity for these two bursts of  $(3.6 \pm 0.4) \times 10^{38} \text{ ergs}^{-1}$  which is consistent with the Eddington luminosity for a  $1.4M_{\odot}$  and 10 km radius neutron star with hydrogen-poor matter (Kuulkers et al. 2002). The other bursts have lower peak fluxes. Burst 3 has a maximum radius close to 20 km and exhibits a temperature drop of 0.8 keV. Bursts 2, 6 and 7 show weak evidence of radius expansion with temperature drops of 0.4-0.7 keV but radius expansion of less than 20 km. Bursts 4, 8 and 9 show no evidence of radius expansion, no temperature drops, and decay more slowly than the other bursts.

Using high time resolution data (merged event lists from the event and burst catcher modes) with no energy selection, we computed power spectra for overlapping 3 s intervals of data, with 0.25 s between the starts of successive intervals, and searched for excess power in the range 100-1000 Hz. We found oscillations in burst 9, with a maximum Leahy normalized power of 38.7 at a frequency of 409.7 Hz, occurring in the burst decay about 5 s after the burst peak. Given 2700 independent frequencies in the 900 Hz interval searched, the signal power corresponds to a probability of chance occurrence of  $1.1 \times 10^{-5}$ , equivalent to a  $4.4\sigma$  detection. The dynamical power spectrum is shown in Fig. 2. The peak rms amplitude of the oscillation is near 6%. Burst 9 is one of the two dimmest bursts and has the longest duration and exponential decay time.

#### 4. Persistent emission

We analyzed the persistent emission following the procedures described in Kaaret et al. (2002). We used only data from PCU2 because this PCU was on during all of the observations. PCU0 was also on during all observations, but a fully reliable background model for PCU0 subsequent to the loss of its propane layer is not available. The PCA light curve shows a high level of variability, up to 80% within one day. An X-ray color-color diagram is shown in Fig. 3 with each point representing a 256 s integration. The points lie mainly in a single cluster, except for a few with low soft colors. A power spectrum for all of the data with soft color above 1.5 is shown in Fig. 4. The power spectrum has very low frequency noise and a so-called high frequency noise component as typically seen from atoll sources in the lower banana state (van der Klis 1995). The solid line superimposed on the data is a fitted model consisting of the sum of a low-frequency powerlaw,  $\nu^{\gamma}$  with  $\gamma = -2.24$ , for the very low frequency noise and an exponentially cutoff powerlaw,  $\nu^{\gamma} e^{-\nu/\nu_{cut}}$  with  $\gamma = 0.92$  and  $\nu_{cut} = 14.5 \text{ Hz}$ . The RMS fraction is 5.7% in the 0.1-100 Hz range. The points with soft color below 1.5 have the lowest count rates and are from a single, contiguous time interval. A power spectrum of these data does not appear to have the very low frequency noise component, which would be consistent with identification as the island state. The RMS fraction is about 5% in the 0.1-100 Hz range.

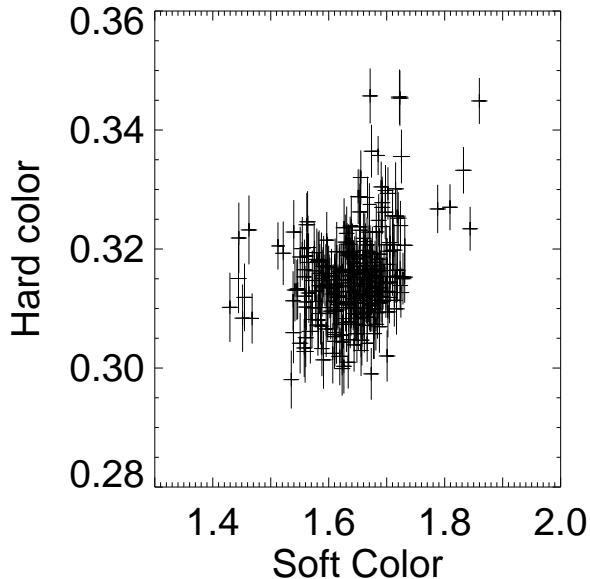


Fig. 3.— Color-color diagram of the persistent emission. Each point represents 256 s of data. The hard color is defined as the count rate in the 9.7–16 keV band divided that in the 6.4–9.7 keV band; the soft color is the 4.0–6.4 keV band rate divided by the 2.6–4.0 keV band rate.

We searched for high frequency QPOs in each uninterrupted RXTE observation window and in combinations of the various data segments, including the sum of the island state data. We calculated averages of 2 s power spectra for all PCA events (2–60 keV) and for events in the 4.7–20.8 keV energy band. We included events from all PCUs on during each observation. We did not find any statistically significant signals.

## 5. Discussion

Our discovery of burst oscillations from the X-ray transient in NGC 6440 adds another source to the 10 sources previously known to exhibit burst oscillations. As described above, X-ray burst oscillation sources form two classes: “slow oscillators” versus “fast oscillators” with the distinction being whether the burst oscillation frequency is close to once or twice the frequency difference of the kHz QPOs in the persistent emission (White & Zhang 1997). The phenomenology of the fast and slow oscillators is different with the fast oscillators being much more likely to produce burst oscillations

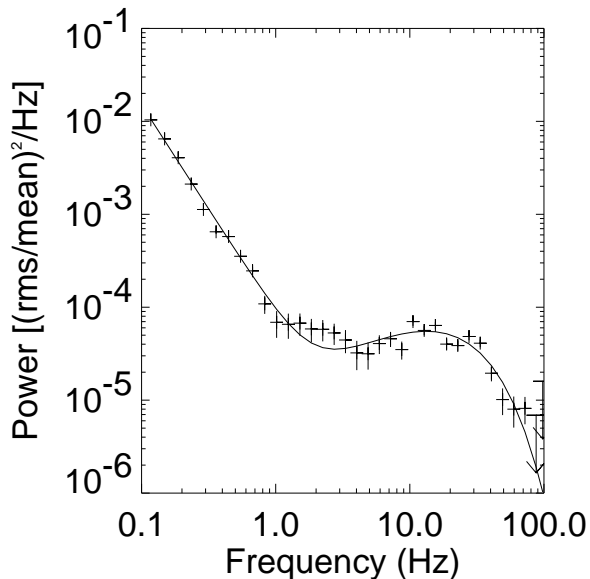


Fig. 4.— Low frequency power spectrum for all observations with soft color above 1.5. The power is RMS normalized. The solid line is a fitted curve described in the text.

in photospheric radius expansion bursts which indicates that there is a physical difference between the two classes (Muno et al. 2001). If the kHz QPO frequency difference is close to the spin frequency of the neutron star, then the slow oscillators produce signals at close to the spin frequency and the fast oscillators at twice the spin frequency.

The fast oscillators have frequencies in the range 521–620 Hz, while the slow oscillators have frequencies in the range 270–363 Hz. The 410 Hz burst oscillation frequency of SAX J1748.9–2021 lies between the two classes. The detection of oscillations during a non-radius expansion burst and the absence of detections in radius expansion bursts is more consistent with the phenomenology of the slow oscillators. However, conclusive assignment of the source to either class must wait until kHz QPOs are detected in the persistent emission. If SAX J1748.9–2021 is a slow oscillator, then it has the highest frequency of any of the slow oscillators and the highest inferred spin frequency of any burst source, but it is slower than the spin frequency of the millisecond X-ray pulsar XTE J1751–305 (Markwardt et al. 2002). If it is a fast oscillator, it has the lowest frequency of any of the fast oscillators and the lowest inferred

spin frequency of any burst source, but it is faster than the millisecond X-ray pulsar XTE J0929-314 (Galloway et al. 2002).

The dichotomy between slow and fast oscillators may be related to the magnetic field configuration of the neutron star. Diametrically opposed magnetic poles provide a natural means to produce oscillations with once or twice the spin frequency. However, the low upper limits placed on the subharmonic for fast burst oscillators are a serious problem for models containing two diametrically opposite hot spots because of the high degree of symmetry required (Muno et al. 2002). The problem is particularly severe when oscillations are detected early in the burst rise because nearly simultaneous ignition of the hot spots would be required.

The evolution of the magnetic field of a neutron star which is spinning-up or down is determined by interactions between superfluid neutrons and superconducting protons within the stellar core (Anderson & Itoh 1975). For a spinning-up star, quantized magnetic flux tubes in the superconducting core move inwards towards the rotation axis (Ruderman 1991). For the NS-LMXBs of interest here, it is likely that sufficient accretion has occurred during spin-up so that the neutron star crust has been replaced several times, giving a corresponding movement of the surface magnetic fields even if neither eddy current dissipation nor creep in the crust has been effective. Since accretion is still occurring, the surface magnetic field emerging from the crust should closely follow the configuration of the core magnetic field.

For the case where all of the emerging magnetic flux returns to the same spin hemisphere, the magnetic flux is squeezed into a small polar cap where the spin axis intersects the crust (Chen et al. 1998). For spin-up from periods near 10 s to periods of milliseconds, both the north and south magnetic poles move close to one rotational pole and the net magnetic dipole field becomes nearly orthogonal to the rotation axis – an orthogonal rotator. The local surface magnetic field strength within the magnetic polar cap is then much higher than the dipole field, typically  $10^{11} - 10^{12}$  G for a dipole field of  $10^8$  G. For the case where flux returns in the opposite hemisphere, the magnetic field is confined to small polar caps at the north and south spin poles. The dipole magnetic field in

this spun-up configuration is oriented nearly parallel to the spin axis – an aligned rotator.

Radio millisecond pulsars (MSPs) are similar to NS-LMXBs, indeed they may be the descendants of the NS-LMXBs, in that they have experienced significant spin-up subsequent to their formation. The orientation of the magnetic field in radio pulsars can be constrained using pulse profile and polarization measurements. The fraction of MSPs in the Galactic disk which are either orthogonal rotators or nearly aligned rotators (exactly aligned rotators would not be pulsars, so there must be a slight offset,  $\sim 20^\circ$ , of the magnetic field from the rotation axis) is significantly higher than for canonical pulsars (Xilouris et al. 1998). Chen et al. (1998) showed that this overabundance of orthogonal and nearly aligned rotators in MSPs can be understood as a consequence of the magnetic field evolution of a neutron star with a superfluid and superconducting core, as described above. The orthogonal and nearly aligned MSPs represent the two endpoints of the magnetic field evolution of a spun-up neutron star.

The magnetic field configuration in LMXBs should be even more tightly compressed towards the rotation poles than in MSPs because in LMXBs the neutron star is still actively accreting and spinning up. The same physical processes which cause the migration of the magnetic poles toward the rotation axis during spin up cause migration away from the rotation axis during spin down. Because MSPs are spinning down, some motion of the magnetic field away from the poles has occurred (the magnitude of the motion is small, since the magnitude of the spin down is small compared to that of the spin up), thereby decreasing the level of symmetry between the poles.

It is interesting to speculate that the same dichotomy may apply to NS-LMXBs. The orthogonal rotator geometry provides a natural means to produce oscillations at twice the spin frequency, while a slightly misaligned parallel rotator would produce oscillations at the spin frequency. The dichotomy between the fast and slow burst oscillators would then be related to physical differences between the magnetic field configurations of the neutron stars.

The magnetic field geometry of orthogonal rotators would produce a high degree of symmetry between the two magnetic poles which would be

located very close to each other. This would naturally suppress the signal at the 1/2 subharmonic, i.e. the spin frequency, in the fast oscillators and allow nearly simultaneous ignition since the two poles are located very close together. Chen et al. (1993) estimate that spin up from 10 s to millisecond periods compresses the magnetic field into a region with a radius of about  $10^4$  cm around the spin axis. For a typical neutron star radius of  $10^6$  cm, the poles would then be less than  $1^\circ$  from the spin axis and be antipodal within  $2^\circ$  as Muno et al. (2002) conclude is required to explain the lack of harmonics and sub-harmonics in burst oscillations. The requirement that there be no more than 2% difference in the relative brightness of the two poles in the main and decaying portions of bursts (Muno et al. 2002) is more difficult to address, but the high degree of symmetry between the two poles and their close location for orthogonal rotators suggest that such uniformity may be achieved several rotation periods after ignition of the burst.

We greatly appreciate the assistance by the duty scientists of the BeppoSAX Science Operations Center in the near to real-time WFC data analysis and the efforts of the RXTE team, particularly Jean Swank and Evan Smith, in performing these target of opportunity observations. PK thanks Mal Ruderman for useful discussions and acknowledges partial support from NASA grant NAG5-7405. JZ acknowledges financial support from the Netherlands Organization for Scientific Research (NWO).

## REFERENCES

- Alpar, M.A., Cheng, A.F., Ruderman, M. A., & Shaham, J. 1982, *Nature*, 300, 728
- Anderson, P. & Itoh, N. 1975, *Nature*, 256, 25
- Bildsten, L. 1998, *ApJ*, 501, L89
- Bradt, H.V., Rothschild, R.E., & Swank, J.H. 1993, *A&AS*, 97, 355
- Burderi, L. et al. 2001, *ApJ*, 560, L71
- Chen, K. & Ruderman, M. 1993, *ApJ*, 408, 179
- Chen, K., Ruderman, M., & Zhu, T. 1998, *ApJ*, 493, 397
- Forman, W., Jones, C., & Tananbaum, H. 1976, *ApJ*, 207, L25
- Galloway, D.K., Chakrabarty, D., Morgan, E.H., & Remillard, R.A. 2002, *ApJ*, 576, L137
- Glendenning, N.K. & Weber, F. 2001, *ApJ*, 559, L119
- in 't Zand, J.J.M. et al. 1999, *A&A*, 345, 100
- in 't Zand, J.J.M., van Kerkwijk, M.H., Pooley, D., Verbunt, F., Wijnands, R., & Lewin, W.H.G. 2001, *ApJ*, 563, L41
- Kaaret, P., in 't Zand, J.J.M., Heise, J., & Tomsick, J.A. 2002, *ApJ*, 575, 1018
- Kuulkers, E., den Hartog, P.R., in 't Zand, J.J.M., Verbunt, F.W.M., Harris, W.E., & Cocchi, M. 2002, *A&A*, in press, astro-ph/0212028
- Lewin, W.H.G., van Paradijs, J., & Taam, R.E. 1995, in *X-Ray Binaries*, ed. W.H.G. Lewin, J. van Paradijs, & E.P.J. van den Heuvel (Cambridge: Cambridge Univ. Press), 175
- Markert, T.H., Backman, D.E., Canizares, C.R., Clark, G.W., Levine, A.M. 1975, *Nature*, 257, 32
- Markwardt, C.B., Swank, J.H., Strohmayer, T.E., in 't Zand, J.J.M., & Marshall, F.E. 2002, *ApJ*, 575, L21
- Muno, M.P., Chakrabarty, D., Galloway, D.K., & Savlov, P. 2001, *ApJ*, 553, L157
- Muno, M.P., Ozel, F., & Chakrabarty, D. 2002, *ApJ*, 581, 550
- Ortolani, S., Barbuy, B., & Bica, E. 1994, *A&AS*, 108, 653
- Pooley, D. et al. 2002, *ApJ*, 573, 184
- Ruderman, M. 1991, *ApJ*, 366, 261
- Strohmayer, T.E., Zhang, W., Swank, J.H., Smale, A., Titarchuk, L., Day, C., & Lee, U. 1996, *ApJ*, 469, L9
- Strohmayer, T.E. & Markwardt, C.B. 2002, *ApJ*, 577, 337
- Tomsick, J.A., Kaaret, P., Kroeger, R.A., & Remillard, R.A. 1999, *ApJ*, 512, 892

- van der Klis, M. 1995, in X-Ray Binaries, ed. W.H.G. Lewin, J. van Paradijs, & E.P.J. van den Heuvel (Cambridge: Cambridge Univ. Press), 252
- Verbunt, F., van Kerkwijk, M.H., in 't Zand, J.J.M., Heise, J. 2000, A&A, 359, 960
- White, N.E. & Zhang, W. 1997, ApJ, 490, L87
- Xilouris, K.M., Kramer, M., Jessner, A., von Hoensbroech, A., Lorimer, D., Wielebinski, R., Wolszczan, A., & Camilo, F. 1998, ApJ, 501, 286